Performance improvement of photovoltaic cells using night radiative cooling technology in a PV/T collector

Abdelkabir Zaite, Naoual Belouaggadia, Cherifa Abid, Mohammed Ezzine

Performance improvement of photovoltaic cells using night radiative cooling technology in a PV/T collector

Abdelkabir ZAITE[1*], Naoual BELOUAGGADIA[2,], Cherifa ABID[3], and Mohammed EZZINE[4]

[1]Laboratory of Engineering and Materials (LIMAT), Faculty of Sciences Ben M'Sik, Hassan II University of Casablanca, Morocco.
[2]Laboratory of signals, distributed systems and artificial Intelligence, ENSET, Hassan II University, Mohammedia, Morocco.
[3]Aix Marseille Univ, CNRS, IUSTI, Marseille, France
[4]Laboratory of physico-Chemistry of applied Materials (LPCMA), Faculty of Sciences Ben M'Sik, Hassan II University of Casablanca, Morocco.

Abstract: The solar radiation absorbed by the photovoltaic thermal systems and not transformed into electricity creates a thermal problem that significantly influences the reliability and efficiency of the photovoltaic cells. In order to passively solve this problem in the hot arid climate, the night radiative cooling technology was proposed in this work, where the water of the system was cooled by circulating in the collector exploiting the proposed technic, and it was used the next day for cooling the photovoltaic cells. For this aim, a mathematical model was developed to present the dynamic thermal behaviour of the PV/T water-based collector, based on the energy balance of its components. Then, the proposed model was validated using the experimental data available in the literature and it was used to study the effect of the glazing and the masse flow rate of water on the cooling performance. The main result indicates that the proposed method reduces the daily temperature of the photovoltaic cells by 3 to 5°C which improves their monthly gain of electrical energy by 5.5% to 6.15% compared with a conventional photovoltaic thermal collector. Consequently, the proposed method allows profiting of the annual potential of the night radiative phenomenon which saved 18.49 kWh as an annual gain of electrical energy.

*correspondent author: E-mail abdelkabir.zaite@gmail.com

Nomenclature:

Q: Energy (j).	ε : Emissivity
P: Power, heat flux (W/m²)	α : Radiative plate absorptivity
T: Temperature (°C, K)	δ : Thickness (m).
G: Solar radiation (W/m²)	
c : Thermal Capacity (j.kg^{-1}.K^{-1})	ρ : Mass density ($kg.m^{-3}$).
h: Heat transfer coefficient (W.m^{-2}.K^{-1})	μ: Dynamic viscosity (Pa.s).
u: Heat transfer coefficient ((W.m^{-2}.K^{-1}))	***Subscripts***

A: Surface (m²)	PV: photovoltaic.
E: Electrical power (W/m²)	am: Ambient.
L : Length (m)	dp: Dew point.
W: Spacing or width (m)	g: glass cover, glazed
d: Diameter (m)	a: Air
Nu: Nusselt number.	p: PV panel.
Re: Reynolds number.	b: Absorber plate
Pr: Prandtl number.	t: Tube bonding.
Ra: Rayleigh number.	w: Water in tube.
V : Control volume (m^3).	i: Insulation layer.
k: Thermal conductivity ($W \cdot m^{-1} \cdot K^{-1}$) .	tk: Storage tank.
g: Acceleration of gravity (9.8 m.s⁻²)	st: Stored in a control volume.
v: Velocity (m/s)	in: inlet.
dt: time step (s)	out: outlet.
dx: space step (m)	ge: Generated.
ΔP: Pressure loss	C: cooling.
Greek symbols	H: heat.
τ : Transmittance	j: number of node in flow direction
$\sigma = 5.67.10^{-8}(W.m^2.K^{-4})$: Stefan-Boltzmann constant	k: iteration counter

1. Introduction:

Solar energy is an alternative source that improves energy consumption and achieves environmental protection, among the technologies of this green source the photovoltaic technology (PV) is one that can be an optimal solution to the consumption problem of electrical energy in buildings. In fact, this technology uses only a small amount of solar radiation to generate electricity, while a large quantity is dispersed as heat, which increases the temperature of photovoltaic cells. The increase of this temperature has a negative effect on the performance and on the reliability of the photovoltaic cells if this energy is not removed [1]. Therefore, a cooling process is necessary to ameliorate the energy performance and reliability of the photovoltaic systems. For this reason, various cooling methods have been addressed in previous studies, such as the airflow cooling method [2][3], the radiative cooling method, where the emissivity of the PV panel is enhanced by selective film or coating [4][5], an active cooling method, based on the flow of water over the PV panel surface [6], and the photovoltaic-thermal collectors (PV/T) methods which are designed to generate heat and electrical energy in parallel. Thus, the used fluid (air, water) allows to cool the PV cells by transferring the thermal energy.

Air-based and water-based PV/T systems have been studied and tested in various studies [7][8][9][10][11][12]. However, the water-based systems have a special ability because of water heat capacity and its significant heat transfer coefficient in the tubes [13][14]. In this device, the glass cover improves thermal efficiency and decreases the electrical one. Besides, the increase in solar radiation and the packing factor enhances exergy efficiency and total energy in laminar and turbulent regimes [15][16]. In addition, the electrical efficiency is also influenced by the increase in the thermal conductive coefficient between the photovoltaic

module and the absorber layer [17]. On the other hand, operating in air-heating or water-heating modes with the same PV/T collector allows better annual efficiency than operating in different modes[18].

In addition to the solar energy technologies, the radiative cooling is another encouraging technology; it is a passive cooling method that uses the atmospheric window ("8-13 µm") to transfer heat from earthly surfaces to the cold space [19]. Historically, this technique was used for the building's cooling and freezing of the water [20]. In fact, radiative cooling takes advantage of low sky temperature to reduce the temperature of the used system [21]. However, it can be listed two techniques of radiative cooling depending on the working time, daytime and night-time. For daytime, the most important parameters are a high emissivity in the infrared atmospheric window band (8–13 µm), and an almost perfect reflection in the near-infrared and visible spectrum (0.3–3 µm). Besides, the radiative coolers can reach important solar reflectivity via exploiting porous structures or high reflective metal. For the night-time application, the previous theoretical and experimental studies indicate that the materials characterized by a high emissivity in the infrared domain are more performing [22][23][24][25].

Recently, radiative cooling and solar energy technologies have been combined in the same system. in this context, an uncovered PV/T collector was utilised to cool a hot storage tank by exploiting the night radiative cooling technology [26]. Furthermore, a new collector was developed by Mingke Hu [27][28][29]to integrate the solar heating and the radiative cooling technologies, this system has shown a good performance for solar heating and radiative cooling by using a composite surface. However, the cooling power rises with an increase in the insulation thickness and the flow rate and it reduces with the increase in wind speed. In the same context, a new design was proposed by Sergei Vall et al. [30][31]. They found that the minimum requirement of cooling and domestic hot water was achieved 25 % and 75 % respectively for single-family, multi-family, and hotel building typologies in some cities.

From the presented literature, firstly, the heating of the photovoltaic cells due to solar radiation is a negative factor that classified among the main problems of their reliability and efficiency. Then, it is well-know also that the night radiative cooling technique was usually used for air conditioning using different systems, while the annual presence of the phenomenon exploited on this technique motivates us to propose another possible application, which can allow profiting of the maximum possible of its cooling potential. Therefore, we have proposed to use this technique for improving the reliability and electrical performance of photovoltaic cells. We have used an unglazed photovoltaic thermal (PV/T) collector for this purpose because it provides the combining of both technologies. In order to investigate this aim, a numerical model was developed to present the variations of temperature and energy of the PV/T collector components. Firstly, the proposed model was validated using the experimental data available in the literature[32]. Then, the effect of the mass flow rate of the working fluid and glass cover on the night performance of the PV/T system has been analysed. Next, the proposed process for cooling was realised as follows; the water in the tank is cooled by circulating in the PV/T collector during the night, benefiting from the radiative cooling phenomenon. The next day, it is used to cool the PV cells of the same collector. The obtained results were compared to those obtained by the same PV/T collector without the proposed cooling process. Compared with the previous models, the proposed one is modified to integrate the night radiative cooling

technology in the PV/T collector. On the other hand, it provides information on the cooling performances and the temperature of each component in the used system including the water in the tank.

2. Method and mathematical model of the PV/T collector:

2.1. Method

The dispersion of the solar radiation as a heat in the PV cells has generally an impact on their reliability and efficiency. Indeed, a part of the solar radiation is not transformed into electrical energy but contributes to an increase of the PV collector temperature which provokes a reduction of its performance. Therefore, the photovoltaic thermal (PV/T) systems have been proposed as a method to reduce this impact, in the PV/T collector, the working fluid (water or air) diminishes the PV cells temperature by transferring a part of the heat absorbed from the solar radiation to the tank, this heat can be used for external applications (thermal heating, domestic hot water etc.) In short, the PV/T collectors are usually used for thermal energy production and electricity generation during the day[10][11][12], and recently, for integrating the night radiative cooling technology [26][33]. This last is a passive cooling method that exploits the atmospheric window for transmitting the thermal infrared radiation of the earthly surfaces toward the sky.

To the best knowledge of the authors, night radiative cooling has been usually integrated in the hybrid systems for thermal cooling or air conditioning, although the period that requires this cooling is limited in the year. Nevertheless, the yearly presence of this phenomenon encourages us to orient its application towards other uses. Therefore, we have proposed to use it for improving the reliability and efficiency of photovoltaic cells in an unglazed PV/T collector. The proposed technique combines the water-cooling method using a photovoltaic thermal collector with the night radiative cooling technology. It promotes the improvement realized by the first method. In addition, it provides an annually profiting of the sky which presents a large tank of cooling. It is investigated as below: at night-time, the water in the tank circulates in the PV/T collector in order to exploit the radiative cooling phenomenon to store a potential of cooling. During the day, instead of using this water for a cooling application, it will be used for cooling of the PV cells in the PV/T collector. This method allowed decreasing the PV cells temperature which improved their monthly reliability and efficiency. The schematic of the proposed technique is shown in Fig.1.
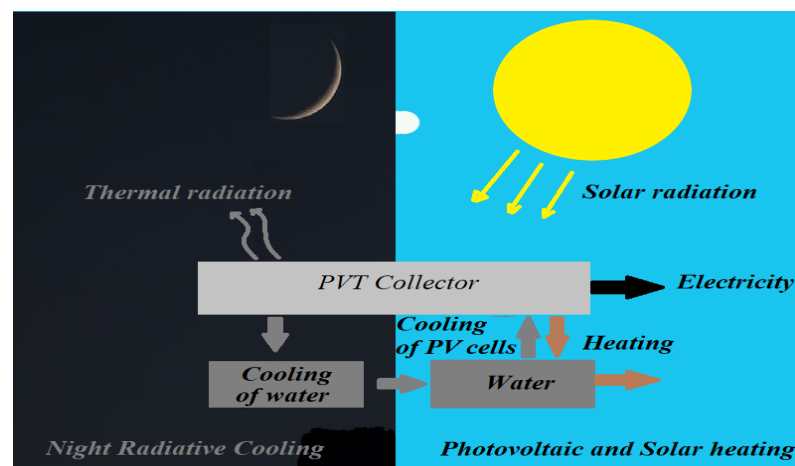
Fig.1. Schematic of night radiative cooling and its use for cooling of the PV cells in a PV/T system.

2.2 mathematical model of the PV/T collector

The PV/T panel used in this study is composed of a photovoltaic panel, an absorber metallic plate which is bonded to ten tubes by a metal bound. In these tubes, the water circulates for evacuating the thermal energy of the indicated collector. The configuration of two principal pipes at the collector extremities allows balancing the flow of water in all tubes. The thermal symmetry plane (TSP) consists of one tube and a part of the absorber and the PV plate of the same width as the average distance between the two adjacent tubes, as shown in Fig. 2.

In the proposed model, the analysed control volume of the indicated panel contains one tube and is subdivided into seven points (glass cover 'g', air gap 'a', PV plate 'p', absorber plate 'b', tube and band 't', water in tube 'w', and the insulation 'i'). It is perpendicular to the water flow direction, Fig. 2.
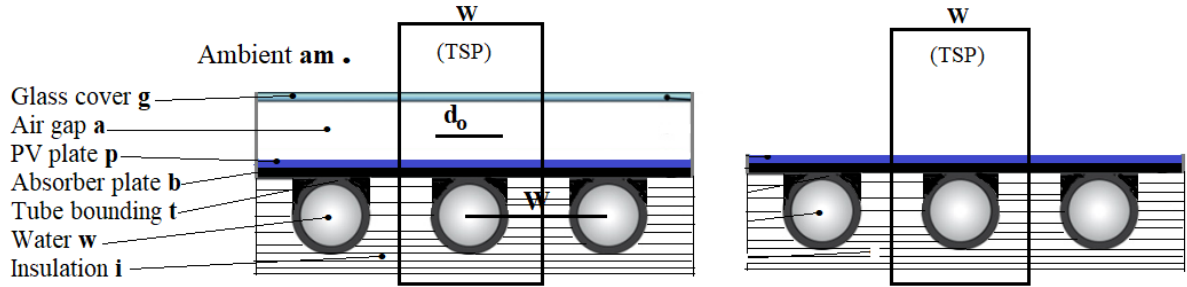

Fig. 2. Glazed and unglazed PV/T collector.

The governing equations for one-dimensional heat transfer are obtained by using the general energy balance for each zone in the analysed control volume. Generally, the energy balance is expressed by the Eq. 1 [1][34]:

$$\frac{dQ_{st}}{dt} = \dot{Q}_{in} - \dot{Q}_{out} + \dot{Q}_{ge} \qquad (1)$$

Where, $\frac{dQ_{st}}{dt}$ presents the stored mechanical and thermal energy, $\dot{Q}_{in}$ and $\dot{Q}_{out}$ are respectively the inlet and outlet energy transport across the control volume, and $\dot{Q}_{ge}$ presents the heat generation rate into the system.

In order to facilitate the model simulation, the follows hypotheses have been assumed:

- The physical properties of the solid components of the PV/T are constant.
- The flow of water is assumed to be uniform in all tubes.
- The impact of edges on the heat transfer is negligible.
- The hourly weather data were calculated by using a typical meteorological year data (TMY2).
- There is no work done in the studied system.
- The changes in the potential and kinetic energies are negligible in the storage tank.
- The inlet water temperature in the collector is considered the same as that of water in the tank.

2.1.1 Temperatures equations

Considering the energy balance (Eq.1) at the thermal symmetry plane of the PV/T collector indicated in Fig. 2 with the surface area A, spacing W and length L; it follows.

- For the glass point g (T_g)

During the day, the glass absorbs an amount of solar radiation and exchanges it by convection with the air gap (present between the glass cover and the absorber) and the external ambient air and by radiation between the sky and PV panel. During the night, the only change in the balance is that the solar radiation becomes zero. Consequently, the energy balance (Eq.1) can be written for the glass point as follows:

$$\rho_g c_g \delta_g \frac{\partial T_g}{\partial t} = \alpha_g G + h_{ag}\left(T_a - T_g\right) + h_{gam}\left(T_{am} - T_g\right) + h_{gsky}\left(T_{sky} - T_g\right) + h_{gp}\left(T_p - T_g\right) \tag{2}$$

Where ρ, δ, c, T, and α, are respectively mass density, thickness, absorptivity, and temperature of the subscripted point, G is the global solar radiation, h_{ag} and h_{gam} are the convective heat transfer coefficients of the couples glass-air gap and glass-ambient air; h_{gsky} and h_{gp} are the radiative heat transfer coefficients of the couples glass-sky and glass-PV panel.

- For the air gap point a (T_a)

The air present in the gap between the glass cover and the PV panel, exchanges heat by natural convection. Thus, the energy balance (Eq.1) is expressed for the air gap point as below:

$$\rho_a c_a \delta_a \frac{\partial T_a}{\partial t} = h_{ag}\left(T_g - T_a\right) + h_{ap}\left(T_p - T_a\right) \tag{3}$$

Where h_{ap} is the convective heat transfer coefficient between the air gap and PV panel.

- For the photovoltaic plate point p (T_p).

Glazed PV/T

The PV panel absorbs the solar radiation transmitted through the glass cover, it transforms a part of it into electrical energy $(E_{pv,g})$ and the other part is transformed into heat $((\tau\alpha)_p G)$. It also exchanges another amount by radiation with the glass cover and by convection with the air gap, and by conduction with the absorber plate and tube. At night, it exchanges the heat transferred by conduction from the absorber plate to the glass by radiation and to the air gap by convection. As a result, for the PV point, the energy balance (Eq.1) can be written as:

$$\rho_p c_p \delta_p \frac{\partial T_p}{\partial t} = h_{gp}\left(T_g - T_p\right) + h_{ap}\left(T_a - T_p\right) + \frac{u_{pb} A_{bp}}{A}(T_b - T_p) + \frac{u_{pt} A_{pt}}{A}(T_t - T_p) + (\tau\alpha)_p G - E_{pv,g} \tag{4}$$

Where, A_{pb}, A_{pt}, u_{pb}, and u_{pt} are respectively the heat transfer areas and coefficients of the components couples PV panel-absorber and PV panel-tube, τ is the glass transmittance, and $E_{pv,g}$ corresponds to the electrical energy produced by the PV panel.

Unglazed PV/T

In this case, we consider the same energy balance of the PV point in the glazed PV/T with removing the glass cover effect and replacing it with the sky, and the air gap with that ambient, considering the forced convection heat transfer added. During the night, it is cooled by transferring an amount of heat energy as infrared radiation towards the sky. So, the energy balance (Eq.1) can be written for the PV point as:

$$\rho_p c_p \delta_p \frac{\partial T_p}{\partial t} = h_{psky}\left(T_{sky} - T_p\right) + h_{pam}\left(T_{am} - T_p\right) + \frac{u_{pb}A_{bp}}{A}(T_b - T_p) + \frac{u_{pt}A_{pt}}{A}(T_t - T_p) + \alpha_p G - E_{pv} \tag{5}$$

- For the absorber plate point **b** (T_b).

The absorber exchanges the heat only by conduction with the PV plate, the tube, and the insulation layer. During the night, it absorbs the heat from the tube and transfers an amount of it by conduction to the PV plate and a small part to the insulation layer. Thus, the energy balance of the absorber point (Eq.1) is written as below:

$$\rho_b c_b V_b \frac{\partial T_b}{\partial t} = u_{pb}A_{pb}\left(T_p - T_b\right) + u_{bt}A_{bt}(T_t - T_b) + u_{bi}A_{bi}\left(T_i - T_b\right) \tag{6}$$

Where V_b is the volume of the absorber in the thermal symmetry plane. A_{bt}, A_{bi}, u_{bt}, and u_{bi} are respectively the heat transfer areas and coefficients of the couples absorber-tube and absorber-insulation.

- For the tube bonding point **t** (T_t).

The tube absorbs the heat from the absorber and PV panel, then it transfers a small quantity of this energy by conduction to the insulation layer, the other one is transmitted to the water by convection. Overnight, it transfers the heat absorbed from the water to the absorber, the PV panel, and the insulation layer. Consequently, the energy balance (Eq.1) can be expressed for the tube bonding point as following:

$$\rho_t c_t V_t \frac{\partial T_t}{\partial t} = u_{bt}A_{bt}(T_b - T_t) + u_{pt}A_{pt}(T_p - T_t) + u_{ti}A_{ti}\left(T_i - T_t\right) + h_{tw}\pi d_{in}L\left(T_t - T_w\right) \tag{7}$$

Where V_t is the volume of the tube, A_{ti} and u_{ti} are respectively, the heat transfer areas and coefficients between the tube and insulations components, h_{tw} is the convective heat transfer coefficient between tube and water, and d_{in} is the inlet diameter of the tube.

- For the water in tube point **w** (T_w).

Considering the properties of water are a function of its temperature, the variation of total energy with time, and the heat exchanged into its control volume, the energy balance (Eq.1) of water point can be written as below:

$$\rho_w c_w A_w \frac{\partial T_w}{\partial t} = \pi d_{in} h_{tw}\left(T_w - T_t\right) - \rho_w c_w A_w v_x \frac{\partial T_w}{\partial x} \tag{8}$$

Where v_x is the water velocity in tube, and A_w is the section of water flow.

- For the insulation point **i** (T_i).

In addition to the heat exchanged with the tube and the absorber plate, the insulation layer transfers an amount of heat to the ambient air by convection. Consequently, for the insulation point the energy balance (Eq. 1) can be written as next:

$$\rho_i c_i V_i \frac{\partial T_i}{\partial t} = u_{it} A_{it} (T_t - T_i) + u_{bi} A_{bi} (T_b - T_i) + u_{iam} A_{iam} (T_{am} - T_i) \tag{9}$$

Where V_i is the volume of insulation in the thermal symmetry plane, u_{iam} is the global heat transfer coefficient between the insulation and the ambient air, and A_{iam} is the external area of insulation.

- The inlet water point (water in the tank) **w,in ($T_{w,in}$)** [35][36]

For the water in the tank, the first law of thermodynamics was applied over the tank control volume with a neglecting of the changes in the potential and kinetic energies and considering the heat exchanged with the ambient air through the tank thickness. Thus, the inlet water temperature variation is written as follows:

$$\rho_{w,in} c_{w,in} V_{tk} \frac{\partial T_{w,in}}{\partial t} = \dot{m}_w c_{w,in} (T_{w,in} - T_{w,out}) + u_{tk} A_{tk} (T_{am} - T_{w,in}) \tag{10}$$

Where V_{tk} is the volume of the tank, $\dot{m}_w$ is the total mass flow rate of water, $T_{w,out}$ is the water temperature at the outlet of the collector, and u_{tk} is the heat loss coefficient at the outside surface of the tank (A_{tk}), including the thermal resistance of the tank insulation.

- Sky temperature

The effective sky temperature is given by the follow equation:

$$T_{sky} = \varepsilon_{sky}^{0.25} T_{am} \tag{11}$$

where ε_{sky} is the sky emissivity, which is calculated using empirical correlation (Eq. 12) as a function of the dew point temperature [19].

$$\varepsilon_{sky} = 0.711 + 0.56 \left(\frac{T_{dp}}{100} \right) + 0.73 \left(\frac{T_{dp}}{100} \right)^2 + 0.0013 cos \left(\frac{2\pi t}{24} \right) \tag{12}$$

Where T_{am} and T_{dp} are the air and dew point temperatures, they are estimated by using the typical meteorological year data (TMY2).

2.1.2 Heat transfer coefficients and surfaces.

The coefficients and areas of heat transfer needed for simulation are presented in Table 1 and Table 2.

Table 1

Different heat transfers coefficients.

Component couple	Transfer mode	Formula

Glass cover –Air gap PV plate-Air gap	Forced-Convection	$$h_{ag} = h_{ap} = \frac{N_{ua}k_a(T_a)}{\delta_a}$$	(13)
Glass cover–Ambient [37]	Mixed-Convection	$$h_{gam} = 3v_w + 2.8 + \frac{N_{ua}k_{am}(T_{am})}{\delta_{am}}$$	(14)
Glass cover-sky [37]	Radiation	$$h_{gsky} = \varepsilon_g \sigma \left(T_g^2 + T_{sky}^2\right)\left(T_g + T_{sky}\right)$$	(15)
Glass cover- PV panel	Radiation	$$h_{gp} = \sigma \left(T_g^2 + T_p^2\right)\left(T_g + T_p\right)\left(\frac{1}{\varepsilon_p} + \frac{1}{\varepsilon_g} - 1\right)^{-1}$$	(16)
PV panel-sky (unglazed)	Radiation	$$h_{psky} = \varepsilon_p \sigma \left(T_p^2 + T_{sky}^2\right)\left(T_p + T_{sky}\right)$$	(17)
PV-Ambient [37] (unglazed)	Mixed-Convection	$$h_{pam} = 3v_w + 2.8 + \frac{N_{ua}k_a(T_{am})}{\delta_{am}}$$	(18)
PV-Absorber [38]	Conduction	$$u_{pb} = \frac{k_{ad}}{\delta_{ad}}$$	(19)
PV-Tube [38]	Conduction	$$u_{pt} = \left(\frac{W}{8k_p} + \frac{\delta_{ad}\delta_p}{k_{ad}d_o}\right)^{-1}$$	(20)
Absorber-insulation [38].	Conduction	$$u_{bi} = \frac{2k_i}{\delta_i}$$	(21)
Absorber-Tube[38].	Conduction	$$u_{bt} = \frac{8k_b}{W - d_o}$$	(22)
Water-Tube [39]	Convection	$$h_{tw} = \frac{N_{uw}k_w(T_w)}{d_{in}}$$	(23)
Insulation-Ambient [38].	Conduction and convection	$$u_{iam} = \left(\frac{\delta_i}{2k_i} + \frac{1}{h_{pam}}\right)^{-1}$$	(24)
Tank-Air	Conduction and mixed-convection	$$u_{tk} = \left(\frac{\delta_{tk}}{2k_{tk}} + \frac{1}{h_{pam}}\right)^{-1}$$	(25)

Where k_{ad} and δ_{ad} are respectively the thermal conductivity and the thickness of the layer between the absorber plate and the photovoltaic cells[38].

Table 2

Different heat transfer areas [38]

Component couple	Area	
PV panel-Absorber	$$A_{bp} = A\left(1 - \frac{d_o}{W}\right)$$	(26)

PV panel-Tube	$A_{pt} = \delta_p L$	(27)
Absorber-Insulation	$A_{bi} = A\left(1 - \dfrac{d_o}{W}\right)$	(28)
Absorber-Tube	$A_{bt} = \delta_b L$	(29)
Insulation-Tube	$A_{it} = \left(\dfrac{\pi + 2}{2}\right) d_o L$	(30)
Water area	$A_w = \dfrac{1}{4}\pi d_{in}^2$	(31)

In order to calculate the forced convective heat transfer coefficients of air, the Nusselt number of air gap and ambient air (N_{ua}) has been calculated using the follow correlations [17]:

If $T_p > T_a$ or $T_p > T_{am}$

$$N_{ua} = 1 + 1.44\left[1 - \frac{1708}{Ra\delta_a \cos(\theta)}\right] * \left[1 - \frac{1708(\sin(\theta))^{1.66}}{Ra\delta_a \cos(\theta)}\right] + \left[\frac{(Ra\delta_a \cos(\theta))^{0.33}}{5830} - 1\right]$$ (32)

If $T_p < T_a$ or $T_p < T_{am}$ [28]

$$N_{ua} = 1 + [0.364\frac{L}{\delta_a}Ra^{0.25} - 1]\sin(\theta)$$ (33)

If $T_p = T_a$, the Nusselt number is equal to zero.

Where Ra and θ are respectively the Rayleigh number and the tilt angle. These expressions are valid for tilt angles (θ) ranging from 0° to 75°.

For the unglazed PV/T the air gap thickness is replaced by the equivalent thickness of ambient air, which is calculated as follows [40]:

$$\delta_{am} = \frac{4LW}{\sqrt{L^2 + W^2}}$$ (34)

The Nusselt number of water flow (N_{uw}) has been calculated utilizing the empirical correlations available in the literature:

For laminar flow[16]

$$N_{uw} = \begin{cases} 1.953\left(\dfrac{Re\,Pr\,d_{in}}{L}\right)^{1/3} & \dfrac{L}{Re\,Pr\,d_{in}} \leq 0.03 \\ 4.364 + \dfrac{0.0722\,Re\,Pr\,d_{in}}{L} & \dfrac{L}{Re\,Pr\,d_{in}} > 0.03 \end{cases}$$ (35)

For turbulent flow [39]:

$$N_{uw} = 0.023\,Re^{0.8}\,Pr^{0.3}$$ (36)

Where Pr and Re are respectively, Prandtl and Reynolds numbers.

The following equations have been used to calculate the thermal physical properties of water [41].

$$\rho_w = -0.003T_w^2 + 1.505T_w + 816.781 \tag{37}$$

$$c_w = -0.0000463T_w^3 + 0.0552T_w^2 - 20.86T_w + 6719.637 \tag{38}$$

$$k_w = -0.000007843T_w^2 + 0.0062T_w - 0.54 \tag{39}$$

$$\mu_w = 0.00002414 \times 10^{\frac{247.8}{T_w - 140}} \tag{40}$$

Where μ_w is the dynamic viscosity of water.

2.1.3   Performance evaluation

The electrical energy and efficiency of the PV cells in the glazed ($E_{pv,g}$) and unglazed (E_{pv}) PV/T collector considering the electrical energy consumed by the pump (P_{pump}) are presented in Table 3:

Table 3

Expressions of the electrical energy and efficiency

Energy	Equation	
Electrical energy of the glazed PV/T collector [18]	$E_{pv,g} = (\alpha\tau)_p G\eta_r r_{pb}\left[1 - B_r(T_p - T_r)\right]$	(41)
Electrical energy of the unglazed PV/T collector[18]	$E_{pv} = \alpha_p G\eta_r r_{pb}\left[1 - B_r(T_p - T_r)\right]$	(42)
Electrical efficiency [16]	$\eta_{pv} = \dfrac{E_{pv} - P_{pump}}{GA_{pv}}$	(43)
Pump power P_{pump} [16]	$P_{pump} = \dfrac{\dot{m}_w \times \Delta P}{\rho_w \times \eta_{pump}}$	(44)

where r_{pb} is the ratio of cell area to interstice area, G is the solar radiation, η_r is the reference cell efficiency at the reference temperature T_r, B_r is the temperature coefficient, and ΔP is the evaluating pressure loss, which is expressed by the follow equation [16]:

$$\Delta P = \rho g\left(L\sin\varphi + \left[\frac{8\dot{m}_w^2}{\rho^2 g\pi^2 d_{in}^4}\left(f\frac{1}{d_{in}} + K_1 + K_2\right)\right]\right) \tag{45}$$

when $L\sin\varphi$ is the vertical distance between inlet and outlet of the collector, K_1 and K_2 are respectively loss coefficient at the inlet and the outlet of the tube and they are considered equal to 0.5 and 1, respectively, and f is the friction coefficient [16][42].

In the PV/T water cooling mode at night, the instantaneous cooling power (P_C) of the system was defined as the heat loss of the water between the outlet and the inlet of the collector and is expressed as [43][44]:

$$P_C(t) = \dot{m}c_w \left(T_{w,in} - T_{w,out} \right)$$ (46)

The instantaneous heating power P_H of the PV/T collector was defined as the heat gained by the working fluid between the outlet and the inlet of the collector, it is given by:

$$P_H = \dot{m}c_w \left(T_{w,out} - T_{w,in} \right)$$ (47)

Thus, the thermal energy efficiency is calculated as follows:

$$\eta_H = \frac{P_H}{GA}$$ (48)

3. Numerical modelling of unglazed PV/T water-based system and experimental validation.

3.1. Numerical modelling of the PV/T water-based collector.

The transient energy balance equations for the various component of the PV/T collector have been resolved using the implicit finite difference method. A control volume was created by defining a theoretical boundary including a physical volume in which the laws of mass and energy conservation were applied. The water flow rate and temperature conditions were considered as the same in all parallel tubes. The partial and time differential equations were discretized by using the Eq.49 and Eq.50.

$$\frac{\partial T}{\partial x} = \frac{T_{j+1}^{t+dt} - T_j^{t+dt}}{dx}$$ (49)

$$\frac{\partial T}{\partial t} = \frac{T_j^{t+dt} - T_j^{t}}{dt}$$ (50)

where T presents the temperature of '*g*' glass cover, '*a*' air gap, '*p*' PV plate, '*b*' absorber plate, '*t*' tube bonding, '*w*' water in tube and '*i*' insulation layer.

j presents the node number in the flow direction (x)

Accordingly, the energy balance equations based on the finite-difference formulation can be written as follows:

$$T_{g,j}^{t+dt} = \beta_g \left[T_{g,j}^{t} + \frac{dt}{\rho_g c_g \delta_g} \left(\alpha_g G + h_{ag} T_a + h_{gam} T_{am} + h_{gsky} T_{sky} + h_{gp} T_p \right) \right]$$ (51)

$$T_{a,j}^{t+dt} = \beta_a \left[T_{a,j}^{t} + \frac{dt}{\rho_a c_a \delta_a} \left(h_{ag} T_g + h_{ap} T_p \right) \right]$$ (52)

Glazed PV/T

$$T_{p,j}^{t+dt} = \beta_{Gp}\left[T_{p,j}^{t} + \frac{dt}{\rho_p c_p \delta_p}\left(h_{pg}T_{g,j}^{t+dt} + h_{ap}T_a^{t+dt} + \frac{u_{pb}A_{bp}}{A}T_{b,j}^{t+dt} + \frac{u_{pt}A_{pt}}{A}T_{t,j}^{t+dt} + (\tau\alpha)_p G^{t+dt} - E_{GPV}^{t+dt}\right)\right] \qquad (53)$$

Unglazed PV/T

$$T_{p,j}^{t+dt} = \beta_p\left[T_{p,j}^{t} + \frac{dt}{\rho_p c_p \delta_p}\left(h_{psky}T_{sky}^{t+dt} + h_{pam}T_{am}^{t+dt} + \frac{u_{pb}A_{bp}}{A}T_{b,j}^{t+dt} + \frac{u_{pt}A_{pt}}{A}T_{t,j}^{t+dt} + \alpha_p G^{t+dt} - E_{PV}^{t+dt}\right)\right] \qquad (54)$$

$$T_{b,j}^{t+dt} = \beta_b\left[T_{b,j}^{t} + \frac{dt}{\rho_b c_b V_b}\left(u_{bp}A_{bp}T_{p,j}^{t+dt} + u_{bt}A_{bt}T_{t,j}^{t+dt} + u_{bi}A_{bi}T_{i,j}^{t+dt}\right)\right] \qquad (55)$$

$$T_{t,j}^{t+dt} = \beta_t\left[T_{t,j}^{t} + \frac{dt}{\rho_t c_t V_t}\left(u_{bt}A_{bt}T_{b,j}^{t+dt} + u_{pt}A_{pt}T_{p,j}^{t+dt} + u_{it}A_{it}T_{i,j}^{t+dt} - h_{tw}\pi d_i L T_{w,j}^{t+dt}\right)\right] \qquad (56)$$

$$T_{w,j}^{t+dt} = \beta_w\left[T_{w,j}^{t} - \frac{\pi d_{in} h_{tw} dt}{\rho_w c_w A_w}T_{t,j}^{t+dt} + \frac{u_x dt}{dx}T_{w,j-1}^{t+dt}\right] \qquad (57)$$

$$T_{i,j}^{t+dt} = \beta_i\left[T_{i,j}^{t} + \frac{u_{it}A_{it}dt}{\rho_i c_i V_i}T_{t,j}^{t+dt} + \frac{u_{ib}A_{ib}dt}{\rho_i c_i V_i}T_{b,j}^{t+dt} + \frac{u_{ia}A_{ia}dt}{\rho_i c_i V_i}T_{am}^{t+dt}\right] \qquad (58)$$

$$T_{w,in}^{t+dt} = T_{w,in}^{t} + dt\frac{\dot{m}_w c_w}{\rho_w c_w V_{tk}}\left(T_{w,out}^{t} - T_{w,in}^{t}\right) + dt\frac{u_{tk}A_{tk}}{\rho_w c_w V_{tk}}\left(T_{am}^{t} - T_{w,in}^{t}\right) \qquad (59)$$

The coefficients β_g, β_a, β_{Gp}, β_p, β_b, β_t, β_w, and β_i are given in appendix A.

The conditions of iteration process for temperatures and stability for the steps of time (dt) and space (dx) are satisfied in the all simulations, as expressed [40][36]:

$$v_w \le \frac{dx}{dt} \qquad (60)$$

$$\left|\frac{T_{j,(k+1)}^{t+dt} - T_{j,(k)}^{t+dt}}{T_{j,(k+1)}^{t+dt}}\right| \le \Omega \qquad (61)$$

Ω is the tolerance of iteration ($\Omega = 10^{-4}$), j represents the correspondent component of PV/T

k is the iteration counter for each single time step.

Fig. 3 presents a flowchart explaining the different steps to solve the mathematical model defined in subsection 3. 1. All physical properties of the PV/T collector can be introduced as inputs. Since all boundary conditions of the proposed model are considered dependent on time, the input data for the numerical code are, the total water mass flow rate, the initial temperature of water in the tank, and the meteorological data including the dew and air temperatures and solar radiation. The current model has been solved using the MATLAB code, and it is used to calculate the temporary temperature variation for any node in the PV/T collector between the initial time (t=0) and the total time (t=10x3600).
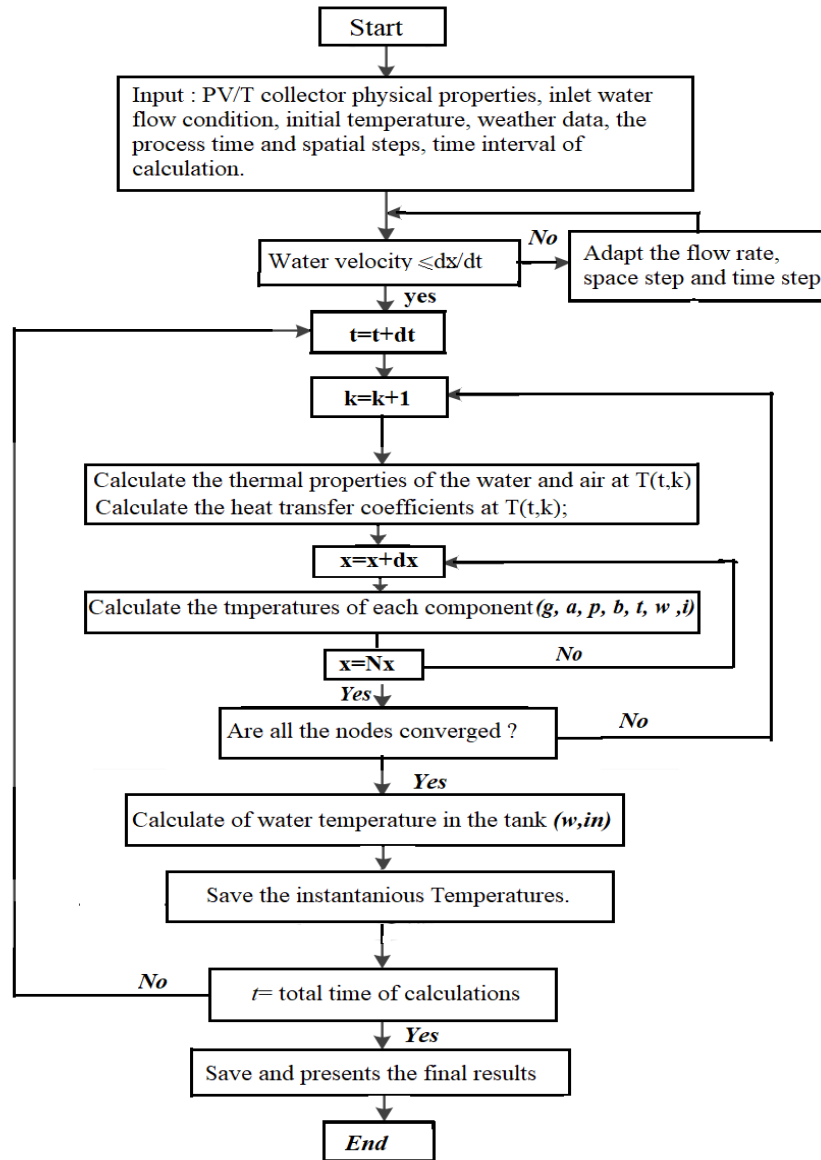
Fig. 3. Code flowchart.

3.2. Experimental validation

The system consists of a photovoltaic-thermal panel (PV/T), a tank of water, and a pump; the parameters of the PV/T panel are illustrated in Table 4. In order to compare the obtained numerical results with that experimental, the numerical and experimental temperatures of the water and the PV module were presented in Fig. 4. Then, the relative error and the root mean square percentage deviation (RMS) have been calculated using the Eq. 62 and Eq. 63[45], and illustrated in Table 5, respectively.

Table 4

Parameters needed for simulations and validation, (PV module: Solarex MSX60, Poly-crystalline silicon) [32][46]

Component	Parameters	Value	Units

Glass cover	Thickness	0.004	m	
	Transmittance	0.92		
	Absorptivity	0.04		
PV Panel	Width	1	m	
	Length	2	m	
	Absorptivity	0.9		
	Emissivity	0.9		
	Thermal conductivity	100	W/(m.K)	
	Reference efficiency	0.11		
	Temperature coefficient	0.0045	K^{-1}	
	Reference temperature	298	K	
Absorber plate	Thickness	0.0005	M	
	Thermal conductivity	310	W/(m.K)	
	Heat capacity	385	J/(kg.K)	
Tube bonding	External diameter	0.01	m	
	Thickness	0.001	m	
	Tube number	10		
	Length	1	m	
	Space between pipes	0.2	m	
Insulation	Thickness	0.03	M	
	Thermal conductivity	0.03	W/(m.K)	
Others	Packing factor	0.9		
	Pump efficiency	0.8		

$$Error(T) = \left| \frac{T_{Sim} - T_{Exp}}{T_{Exp}} \right| * 100 \tag{62}$$

$$RMS = \sqrt{\frac{\sum_{1}^{9} \left[100 * \left(T_{Sim} - T_{Exp} \right) / T_{Exp} \right]^2}{9}} \tag{63}$$

Where T_{Sim} and T_{Exp} correspond to the numerical and experimental temperatures.

From Fig. 4, the PV temperature obtained numerically has the same evolution as the one obtained experimentally with a relative error between 0 and 1.1% which loads to give a RMS of 0.56%, as shown in Table 5. On the other hand, the water temperature shows a slight difference between numerical and experimental models in the first hours due to the assumptions considered in section 2. 2, the relative error is between 0.2% and 3.1% which presents a RMS of 1.6%, as indicated in Table 5. Thus, the temperatures from simulation are in good agreement with that obtained experimentally by Huang and al. [32]. This agreement shows that the proposed model is valid to present the temperature of each component and the energy performance of the PVT-RC water-based collector. It should be mentioned that the linearity of the numerical model is attributed to the hypotheses considered in the section 2. 2.
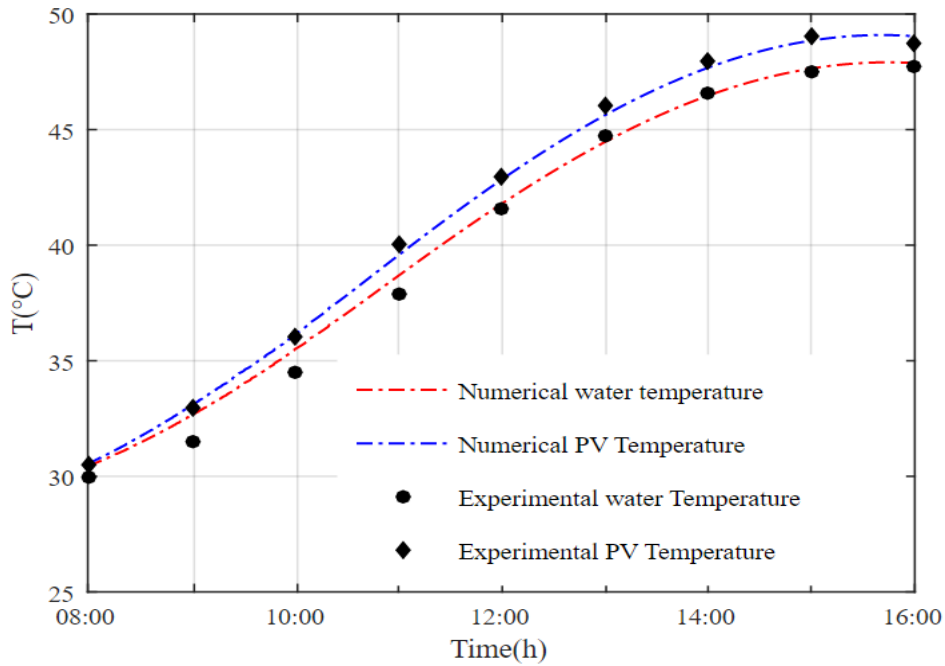
Fig. 4. Comparison between the numerical temperatures of the PV and water with the experimental ones obtained by Huang and al. [32].

Table 5

Relative errors and the root mean square percentage deviation (RMS) between the numerical and experimental models.

	8:00	9:00	10:00	11:00	12:00	13:00	14:00	15:00	16:00	RMS%
Error(T_{pv})%	0	0.03	0.28	1.1	0.25	0.82	0.56	0.26	0.61	0.56
Error(T_w)%	1.3	3.1	2.6	1.68	0.41	0.56	0.3	0.27	0.2	1.6

4. Results and discussion

After validating the present model, the performance of the proposed system has been studied in the arid climate of the city of Ouarzazate. In the first part, a comparison between the night radiative cooling performances obtained by a PV/T with and without glass cover has been discussed. Then, the unglazed PV/T collector has been chosen to integrate the radiative cooling technology, where the influence of the mass flow rate on the evolution of temperatures and cooling power has been presented. The second part is subdivided into two subparts. Firstly, the cooling potential obtained at night is used to cool the PV cells in a PV/T collector during daytime (named PVT-RC). In order to discuss the improvements of the proposed technique, the variations of temperatures, electrical performances, and thermal performances have been presented and compared with these of a PV/T collector without integrating RC technology. Then, the monthly and annual electrical performances of both systems, the electrical energy saved by the PVT-RC system and its ratio have been investigated.

To illustrate, Fig. 5 shows the evolution of the sky, air, and dew point temperatures and the solar radiation during the 14/15 of the month of April in the hot arid climate of Ouarzazate city, in Morocco.
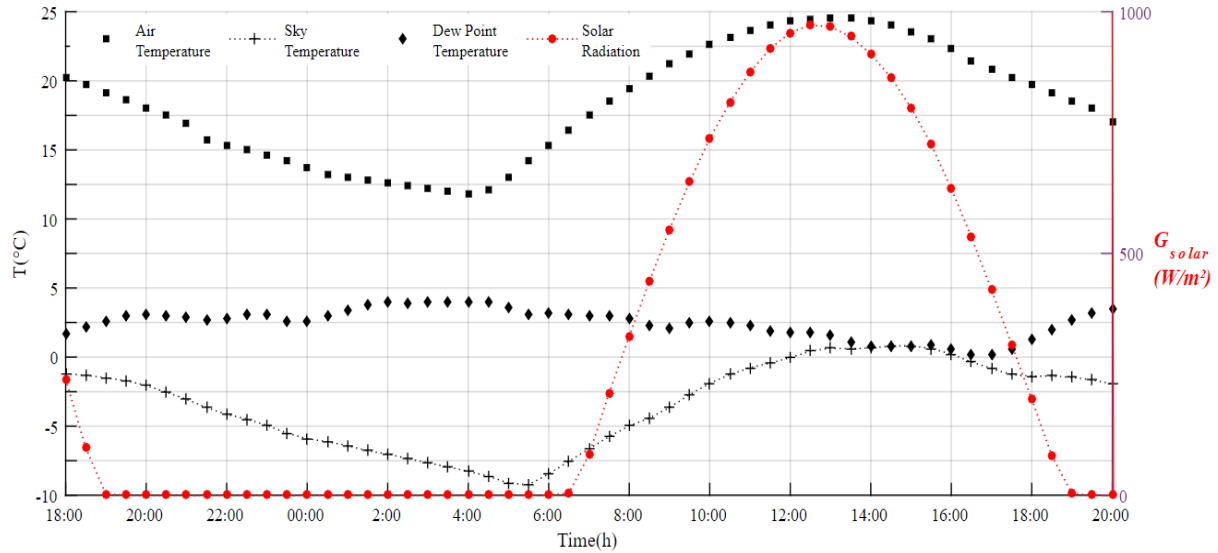
Fig. 5. Variation of air temperature, solar radiation, sky and dew point temperatures during the 14/15 in the month of April.

4.1. Night radiative cooling performance:

The effect of the air temperature, wind velocity and relative humidity on the performance of night radiative cooling technology was investigated in the previous studies [47][29]. Generally, the thermal efficiency and cooling power decrease with the increase in the relative humidity, air temperature, and wind velocity. Besides, the arid climates of Morocco are usually characterized by high ambient temperature during the hot season, which makes its impact more dominant.

4.1.1 Effect of glass cover on the radiative cooling performance

This part analyses the impact of the glass cover on the PV panel temperature and cooling power of the studied PV/T at night, as shown in Fig. 6 (a) and (b). The mass flow rate and storage volume used are 0.01 kg/m³ and 0.15 m³, respectively.

Fig. 6 (a) indicates that the PV panel temperature in the glazed system decreases slowly compared with that obtained in the case without cover, which makes an important difference between the cooling powers presented in Fig. 6 (b). In fact, in the glazed system, the radiative heat exchange is not directly performed between the top surface and the sky, the glass cover acts as a shield to this exchange; this configuration reduces the cooling of the surface due to the greenhouse effect induced by the glass cover. Unlike, in the case of the unglazed system the radiative heat exchange is done directly between the top surface and the sky. Consequently, the unglazed system exploits perfectly the radiative cooling phenomenon compared with that glazed. In brief, the glass cover has a negative impact on the PV/T cooling performance.
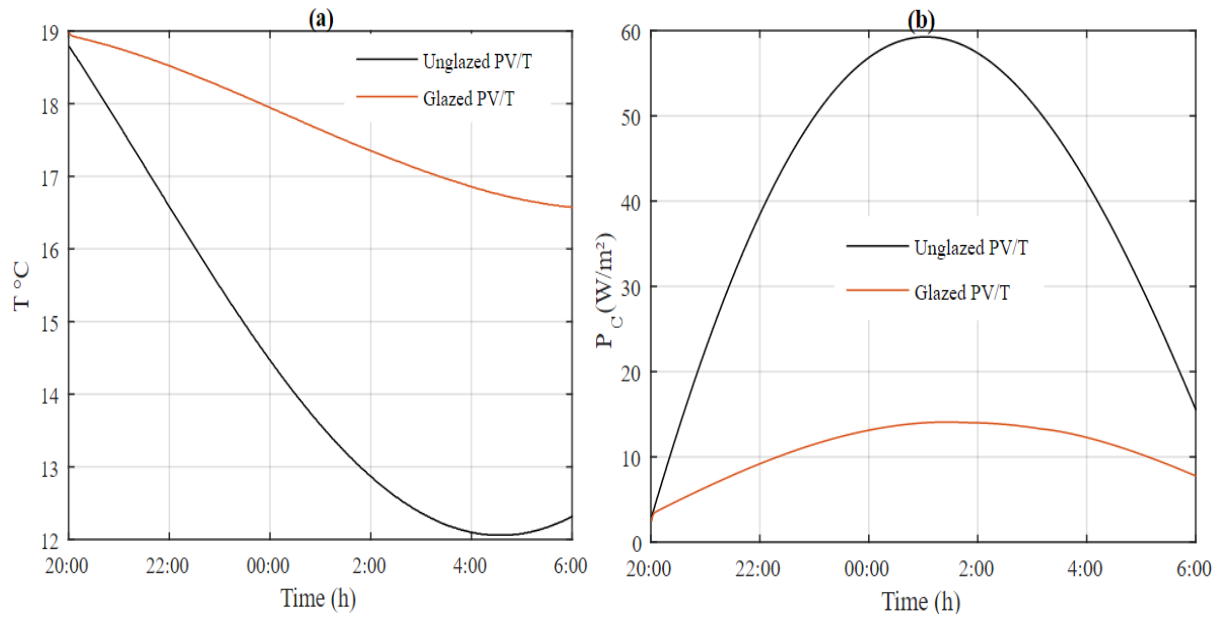
Fig. 6. Variation of PV panel temperature (a) and cooling power of the glazed and unglazed PV/T collector.

4.1.2 *Impact of mass flow rate:*

In this section, the mass flow rate impact on the water temperature in the tank and temperature difference between the inlet and the outlet of the collector (ΔT_{IO}) has been shown in Fig. 7 and Fig. 8, respectively. Then, the variation of cooling power for each mass flow rate has been presented in Fig. 9. The considered initial temperature and volume of water in the tank are respectively: T_0=20 °C and V=0.2 m³.

Fig. 7 shows that the temperatures of water in the tank for various flow rate values. For all the cases, the temperature decreases. One can observe that the temperature decreases for all the considered flow rates; this is due the radiative cooling phenomenon. In addition, the remarkable influence made between the values of 0.01 and 0.04 kg/s is not the same for the other mass flow rates, it becomes less critical step by step, although the amount of the mass flow rate added in each step is the same. On the one hand, this is due to the rise in the number of water cycles between the reservoir and the collector, and the increase in the convective exchange in the tubes of the collector. On the other hand, it is attributed to the variation of energy emitted by the collector with time. It can be seen that the variation mass flow rate has a nonlinear effect on the change in water temperature in the tank.
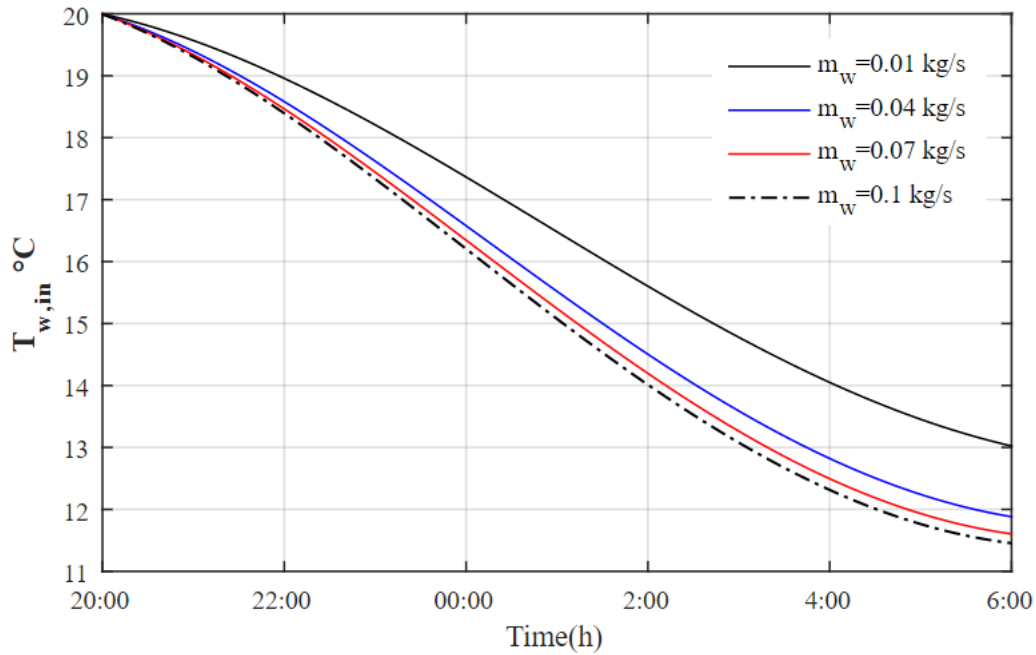
Fig. 7. Variation of water temperatures in the storage tank with time for different mass flow rates.

Fig. 8 indicates that the increase in the mass flow rate is accompanied by a decrease in temperature difference ΔT_{IO}, which is low in the first and last hours, and maximal at midnight for all cases because of the emitted energy evolution of the PV/T. The other reason can be the reduction of heat exchange time between the water and tubes with each added mass flow rate.
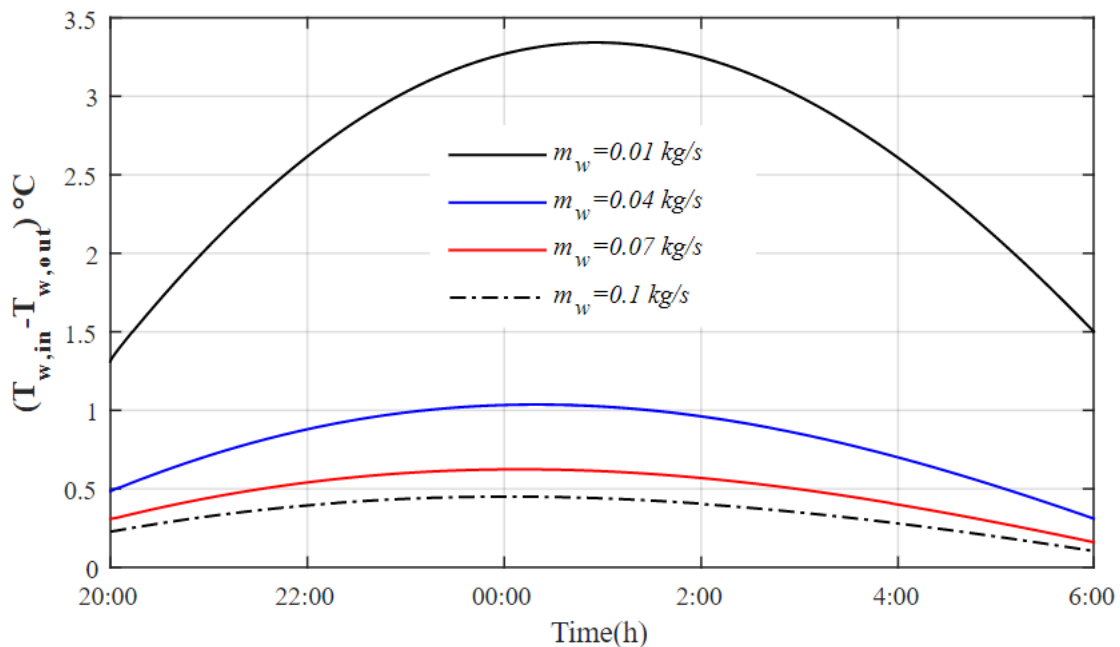

Fig. 8. Variation of the temperature difference ΔT_{IO} with time for different mass flow rates.

On Fig. 9 are plotted the variation of the cooling power versus time for different mass flow rates. The increase in the mass flow rate improves nonlinearly the cooling performance. On the one hand, it is more influential at midnight because of the temperature difference (ΔT_{IO})

variation. On the other hand, the small mass flow rate presents a high power in the last hour because it is characterized by the maximum temperature difference (ΔT_{IO}), which can be more influential than the increment of mass flow rate.
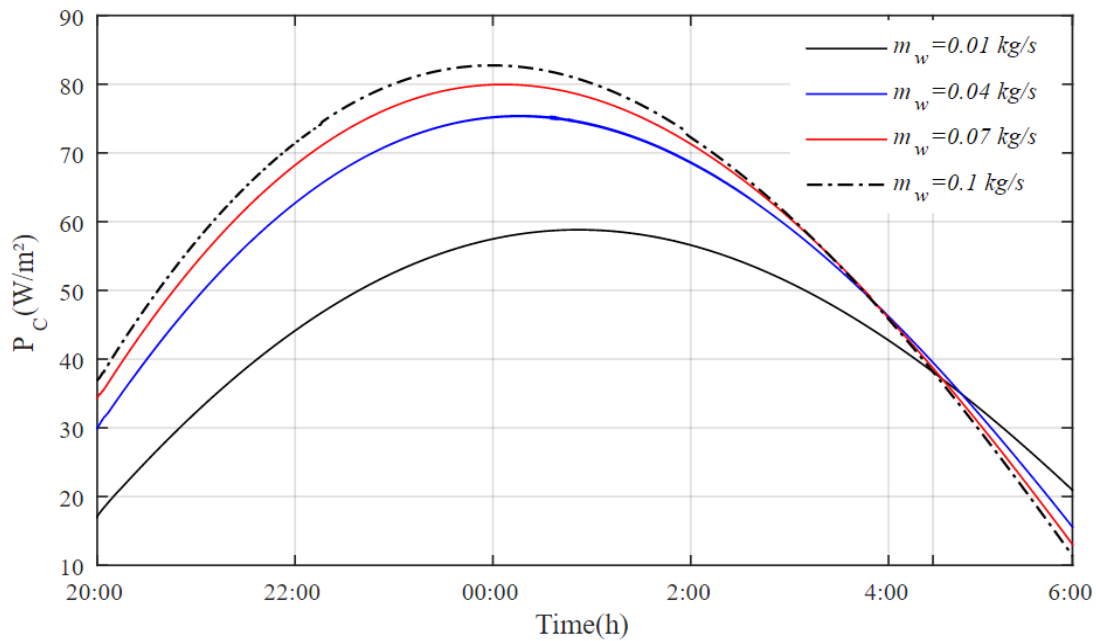

Fig. 9. Variation of cooling power versus time for different mass flow rates.

As a result, the increase in the mass flow rate is a favourable factor to improve the cooling performance when the lost radiative energy of the PV/T collector is high. However, it is accompanied by a decrease in the temperature difference, this last can influence negatively on the cooling power in the last hour at night.

4.2. Diurnal improve of the PV/T system:

In this part, the night radiative cooling technology has been used to improve the electrical performance of the PV/T system. For this aim, two tanks with the same volume of water have been used. The first includes the water with a temperature of 12 °C (named PVT-RC); it was cooled during the night by exploiting the radiative cooling technology. The second includes the water under normal conditions with a temperature of 20 °C (named PV/T). The considered mass flow rate and volume used in this part are 0.025 kg/s and 0.2 m³, respectively.

Fig. 10 shows the variation of the PV panel temperatures versus time for the PVT-RC and PV/T systems. First, the temperatures increase in the first hours. Then, they reach 42 °C and 45 °C for PVT-RC and PV/T systems, respectively. Besides, the result highlights that the integrating of the night radiative cooling technology in the studied system allows reducing the heat of the PV panel, which improves its reliability and efficiency.
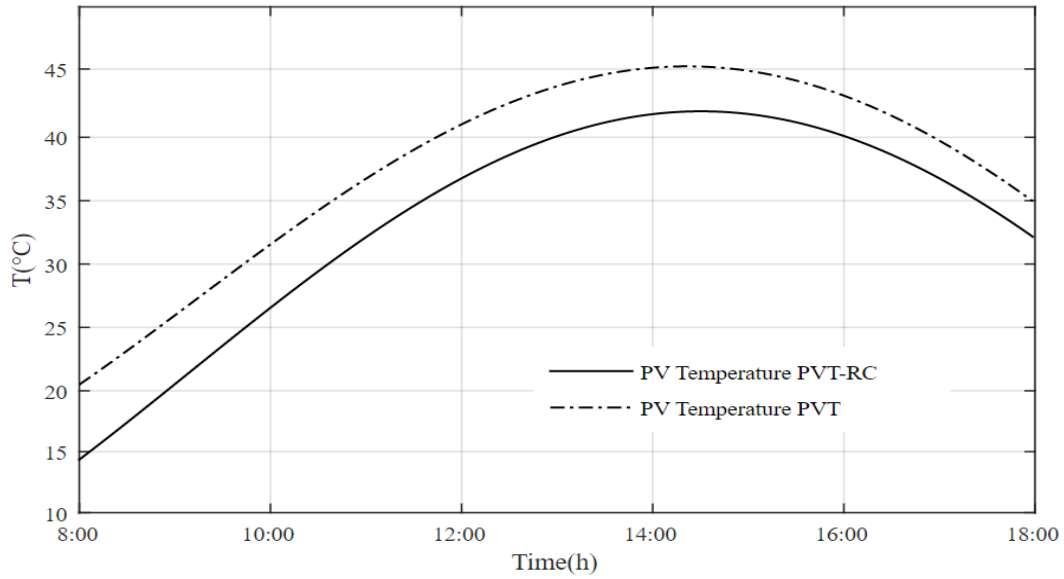
Fig. 10. Variation of average panel temperature with time, against two initial water temperatures in tank.

The variation of water temperatures in the tank is illustrated in Fig. 11. Both temperatures increase gradually with time, reaching 34 °C and 38°C for the PVT-RC and PV/T systems, respectively. Besides, the temperature difference between both decreases slowly with time because of the PV temperature effect. Consequently, the use of night radiative cooling technology allows reducing the water temperature in the tank.
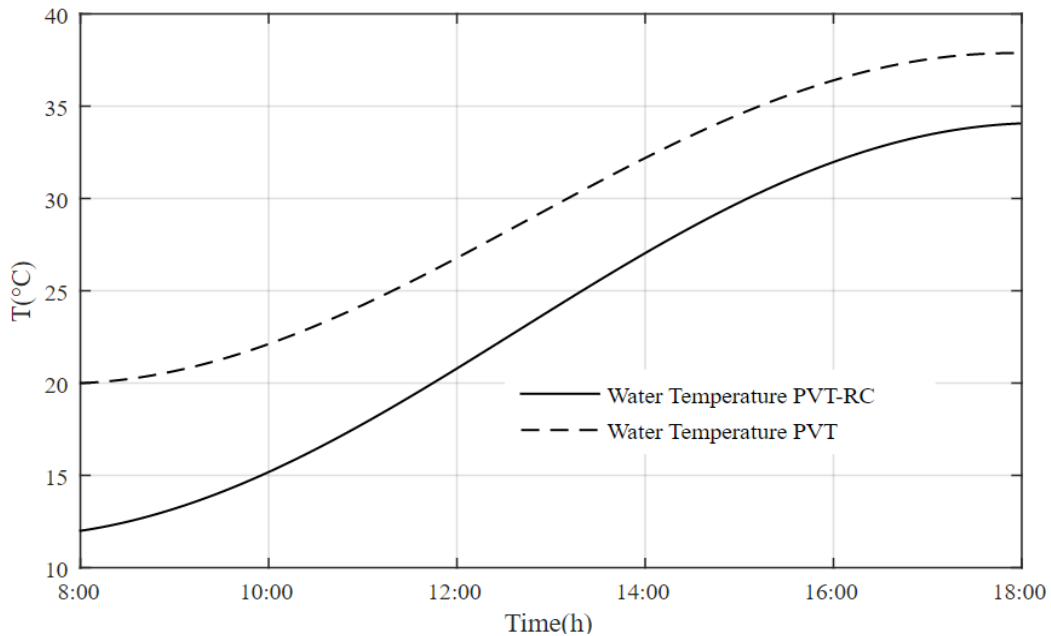

Fig. 11. Variation of water temperature with time for the PV/T and PVT-RC.

Fig. 12 presents the variation of electrical power and efficiency for both systems versus time. The electrical power produced increases, it reaches a maximum of 81 W/m² and 83 W/m² for the PV/T and PVT-RC systems, respectively. Moreover, the electrical efficiency decreases for both cases, because it's more influenced by the solar radiation than the variations of the PV

temperature and electrical power. As a result, the use of water cooled by using the radiative cooling technology presents better electrical performance than that in normal conditions.
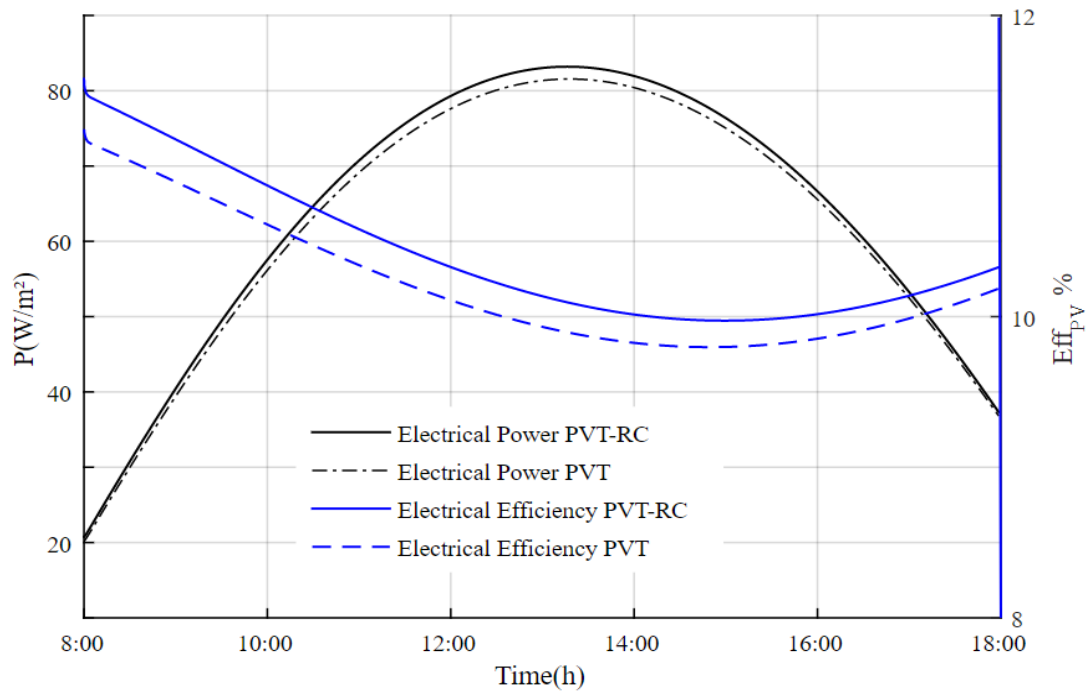

Fig. 12. Variation of electrical power with time for two initial water temperatures.

Fig. 13 shows the variation of thermal power and efficiency for the PVT-RC and PV/T systems versus time. The thermal power takes the same evolution of solar radiation for both systems. The PVT-RC system presents lower heat performance because of the cold water used. Moreover, the thermal efficiencies increase in the first hours of the daytime because of the low values of solar radiation, after, it decreases slowly as a result of the thermal power and solar radiation evolution. In brief, the thermal performance is generally more affected by solar radiation than by other parameters.
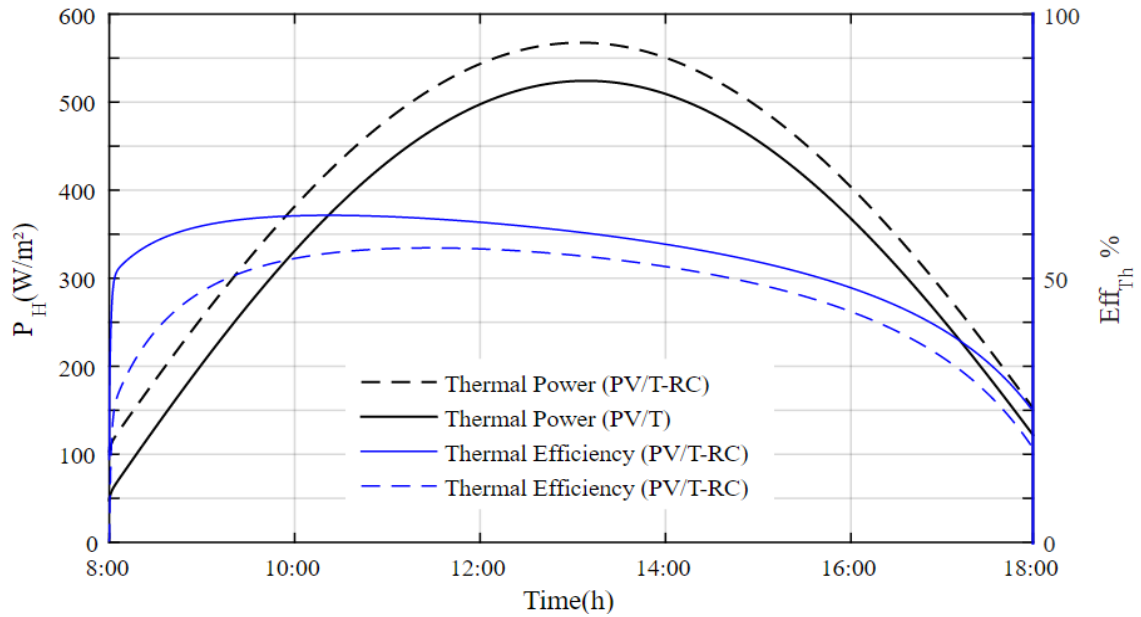
Fig. 13. Variation of thermal power and efficiency of the PVT-RC and PV/T systems with
time.

4.3 Monthly and annual electrical performance:

In order to investigate the monthly and annual improvement of the PV/T electrical performance of the PV/T collector using the night radiative cooling technology, the hourly weather data were provided by typical meteorological year (TMY2) data using Meteonorm and TRNSYS software. A tank volume of $0.2m^3$ was used for both systems. The parameters defined in Table 3 are considered constants. The monthly average air temperature and solar radiation are obtained by using the Meteonorm software, as shown in Fig. 14. The inlet water temperatures of the PV/T and PVT-RC are set continuously equal to the corresponding water temperature in the tank. The periods of the system working in daytime and nocturnal modes are changed based on times sunset and sunrise, which is concluding by the solar radiation values. Then, the monthly electrical energy win is calculated by assembling daily energy gains.
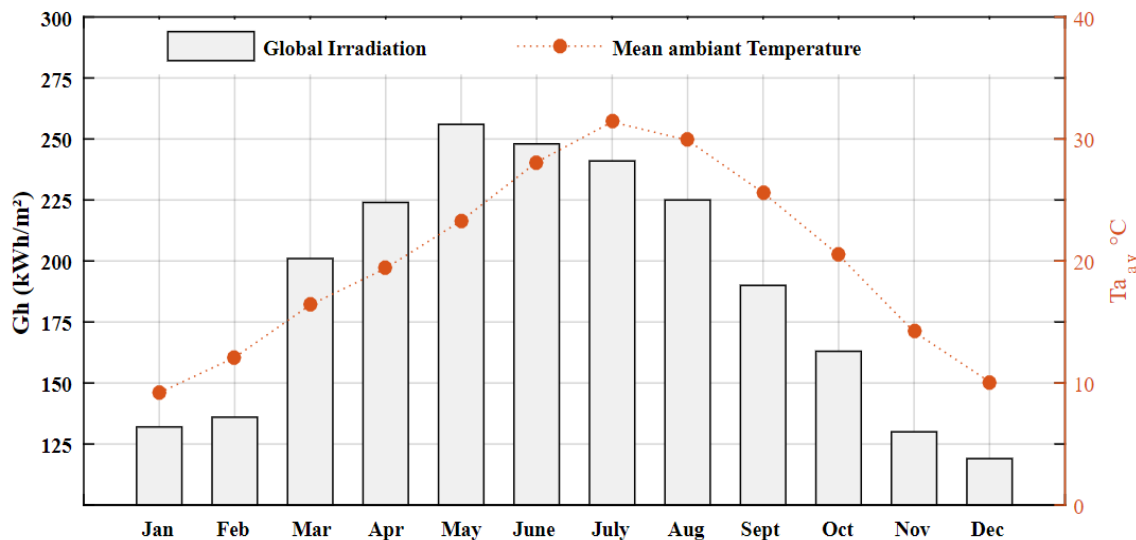
Fig. 14. Global solar radiation and average ambient temperature of the city of Ouarzazate,

Fig. 15 reports the monthly electrical gain for the PVT-RC and PV/T systems. The maximum monthly electrical gain was noted in May because the highest total solar radiation occurs during this month. The minimum value was noted in December as the total solar irradiance is the lowest, as shown in Fig. 15. The monthly and annual performance of the PVT-RC and PV/T with the energy saved (ΔP_e) by the PVT-RC method are reported in Table 6.
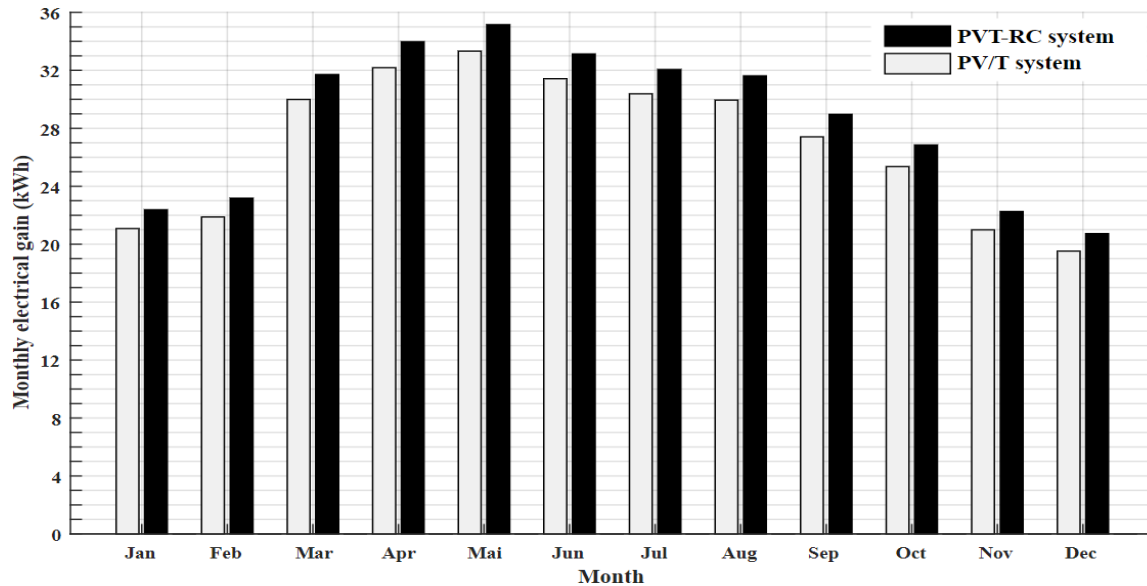

Fig. 15. Monthly performance of the PVT-RC and PV/T systems.

Table 6

Monthly and annual gains of the electrical energy provided by the PVT-RC and PV/T systems and the electrical energy saved by the PVT-RC system.

	PVT-RC P_e (kWh)	PV/T P_e (kWh)	ΔP_e (kWh)
Jan	22.3725	21.0862	1.2863
Feb	23.1826	21.8781	1.30454
Mar	31.7146	29.9972	1.7174
Apr	33.9756	32.1868	1.7888
May	35.1529	33.32712	1.82576
Jun	33.1393	31.42336	1.71594
Jul	32.0621	30.387	1.6751
Aug	31.61516	29.94698	1.66818
Sep	28.96372	27.4082	1.55552
Oct	26.84408	25.35678	1.4873
Nov	22.2529	20.98538	1.26752
Dec	20.73262	19.5306	1.2020
Annual	342.0081	323.5137	18.4944

From Table 6, the saved electrical energy was achieved 1.2 kWh as a minimum value, it was obtained in December as a result of the lowest electrical power noted in this month. The maximum power was 1.82 kWh, and it was achieved in May when the electrical power was also maximum, as shown in Fig. 15. Then, the annual electricity saved by the PVT-RC was 18.49 kWh. Consequently, the night radiative cooling allows improving of the overall performance of the PV cells in the PVT-RC system.

Fig. 16 presents the ratio between the electricity saved by the PVT-RC system ($\mathbf{\Delta}P_e$) and that obtained by the PVT system.
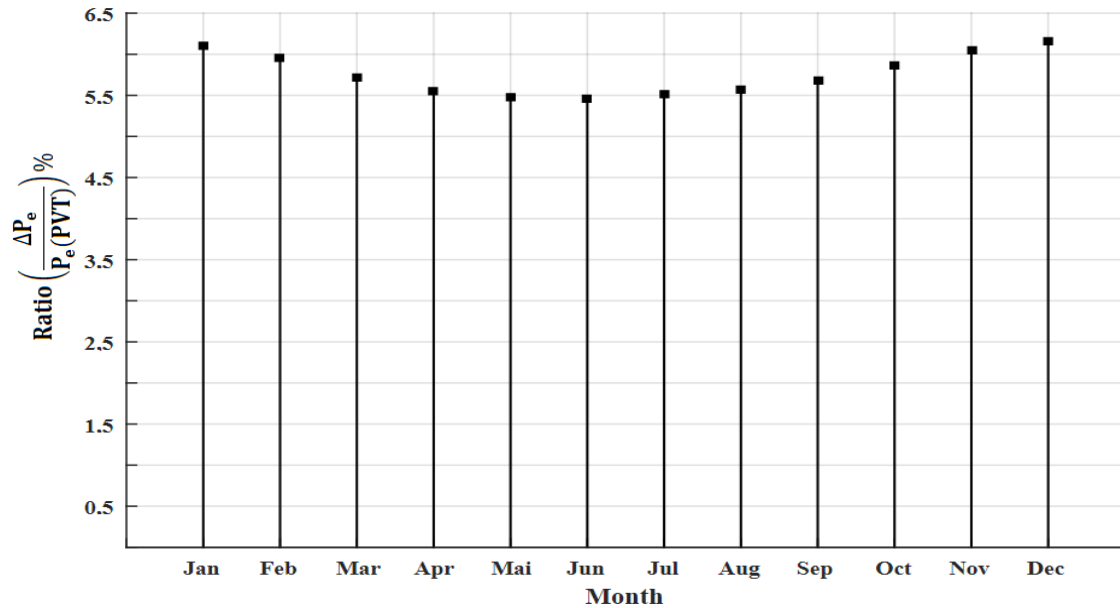

Fig. 16. Ratio between the gain of the electrical energy saved by the PVT-RC system and that generated by the PV/T collector.

According to Fig. 16, the maximum gains of electrical energy gain provided by the PVT-RC system represents 6.15%, 6.10%, 6.01%, and 5.96% of that obtained by the PV/T system in the months of December, January, November, and February, respectively. This is due to that this period was characterised by the lowest air temperature and the highest time of working at night. Likewise, it represents 5.5% to 6% in the other months. It can be seen that the implementation of night radiative cooling provides a significant enhancement of the electrical energy generation of the PV cells in the PVT-RC collector.

As a result, the proposed method of cooling improved the monthly electrical gain of the PV/T collector with an area of 2 m². Likewise, it provided an annual electrical energy gain of 18.49 kWh for a PV/T collector. Thus, it allowed saving almost 5.5% to 6.15% of the monthly electrical energy consumption.

5. Conclusion:

In the present work, the night radiative cooling technology was used as a novel cooling method of photovoltaic cells in a PV/T water-based collector, in order to enhance their reliability and electrical efficiency. The working water was pre-cooled at night exploiting the indicated technology and it was used the next day to decrease the temperature of the PV cells in the used system. The advantage of the proposed method is shown in the reorientation of the use of the night radiative cooling phenomenon and in exploiting its annual presence.

The proposed method of cooling was mathematically realized based on the energy balance of each component in the PV/T collector and of the water in the tank. Then, the proposed model was experimentally validated. Subsequently, the main aims of the present work were investigated in the arid climate of the city of Ouarzazate, Morocco.

From the comparison between the daily results of the PVT and PVT-RC collectors, the proposed method of cooling allowed decreasing the temperature of the photovoltaic cells by 3°C to 5°C in the PVT-RC system, which improved their reliability and electrical efficiency.

The monthly and annual electrical performance analysis shows that the proposed cooling method improved the monthly electrical production of the PV cells by 5.5% to 6.15% compared to its normal production, which allowed saving an annual electrical energy gain of 18.49 kWh.

The proposed method is less efficient for the glazed PV/T collector, because of the negative impact of glass on the infrared radiation emitted by the PV panel, which is the only mechanism that allows cooling the PV/T system by exploiting the radiative cooling phenomenon overnight.

Appendix A:

$$\beta_g = \left(1 + \frac{dt}{\rho_g c_g \delta_g}\left(h_{ag} + h_{gam} + h_{gsky} + h_{gp}\right)\right)^{-1}$$

$$\beta_a = \left(1 + \frac{dt}{\rho_a c_a \delta_a}\left(h_{ap} + h_{ag}\right)\right)^{-1}$$

$$\beta_{Gp} = \left(1 + \frac{dt}{\rho_p c_p \delta_p}\left(h_{pg} + h_{ap} + \frac{u_{pb}A_{bp}}{A} + \frac{u_{pt}A_{pt}}{A}\right)\right)^{-1}$$

$$\beta_p = \left(1 + \frac{dt}{\rho_p c_p \delta_p}\left(h_{psky} + h_{ap} + \frac{u_{pb}A_{bp}}{A} + \frac{u_{pt}A_{pt}}{A}\right)\right)^{-1}$$

$$\beta_b = \left(1 + \frac{dt}{\rho_b c_b V_b}\left(u_{bp}A_{bp} + u_{bt}A_{bt} + u_{bi}A_{bi}\right)\right)^{-1}$$

$$\beta_t = \left(1 + \frac{dt}{\rho_t c_t V_t}\left(u_{bt}A_{bt} + u_{pt}A_{pt} + u_{it}A_{it} - h_{tw}\pi d_i L\right)\right)^{-1}$$

$$\beta_w = \left(1 - \frac{\pi d_{in} h_{tw} dt}{\rho_w c_w A_w} + \frac{u_x dt}{dx}\right)^{-1}$$

$$\beta_i = \left(1 + \frac{dt}{\rho_i c_i V_i}\left(u_{it}A_{it} + u_{ib}A_{ib} + u_{ia}A_{ia}\right)\right)^{-1}$$

References:
[1]   J. A. Duffie (Deceased), W. A. Beckman, and N. Blair, *Solar Engineering of Thermal*

Processes, Photovoltaics and Wind. 2020.

[2]   P. Valeh-E-Sheyda, M. Rahimi, A. Parsamoghadam, and M. M. Masahi, "Using a wind-driven ventilator to enhance a photovoltaic cell power generation," *Energy Build.*, vol. 73, no. 2014, pp. 115–119, 2014, doi: 10.1016/j.enbuild.2013.12.052.

[3]   E. Cuce and P. M. Cuce, "Improving thermodynamic performance parameters of silicon photovoltaic cells via air cooling," *Int. J. Ambient Energy*, vol. 35, no. 4, pp. 193–199, 2014, doi: 10.1080/01430750.2013.793481.

[4]   L. Zhu, A. Raman, K. X. Wang, M. A. Anoma, and S. Fan, "Radiative cooling of solar cells," *Optica*, vol. 1, no. 1, p. 32, 2014, doi: 10.1364/optica.1.000032.

[5]   A. R. Gentle and G. B. Smith, "Is enhanced radiative cooling of solar cell modules worth pursuing?," *Sol. Energy Mater. Sol. Cells*, vol. 150, pp. 39–42, 2016, doi: 10.1016/j.solmat.2016.01.039.

[6]   H. Bahaidarah, A. Subhan, P. Gandhidasan, and S. Rehman, "Performance evaluation of a PV (photovoltaic) module by back surface water cooling for hot climatic conditions," *Energy*, vol. 59, pp. 445–453, 2013, doi: 10.1016/j.energy.2013.07.050.

[7]   T. T. Chow, "A review on photovoltaic/thermal hybrid solar technology," *Appl. Energy*, vol. 87, no. 2, pp. 365–379, 2010, doi: 10.1016/j.apenergy.2009.06.037.

[8]   S. Abdul Hamid, M. Yusof Othman, K. Sopian, and S. H. Zaidi, "An overview of photovoltaic thermal combination (PV/T combi) technology," *Renew. Sustain. Energy Rev.*, vol. 38, pp. 212–222, 2014, doi: 10.1016/j.rser.2014.05.083.

[9]   P. G. Charalambous, G. G. Maidment, S. A. Kalogirou, and K. Yiakoumetti, "Photovoltaic thermal (PV/T) collectors: A review," *Appl. Therm. Eng.*, vol. 27, no. 2–3, pp. 275–286, 2007, doi: 10.1016/j.applthermaleng.2006.06.007.

[10]   Y. Jia, G. Alva, and G. Fang, "Development and applications of photovoltaic – thermal systems : A review," *Renew. Sustain. Energy Rev.*, vol. 102, no. November 2018, pp. 249–265, 2019, doi: 10.1016/j.rser.2018.12.030.

[11]   A. A. Hegazy, "Comparative study of the performances of four photovoltaic/thermal solar air collectors," *Energy Convers. Manag.*, vol. 41, no. 8, pp. 861–881, 2000, doi: 10.1016/S0196-8904(99)00136-3.

[12]   J. K. Tonui and Y. Tripanagnostopoulos, "Improved PV/T solar collectors with heat extraction by forced or natural air circulation," *Renew. Energy*, vol. 32, no. 4, pp. 623–637, 2007, doi: 10.1016/j.renene.2006.03.006.

[13]   H. M. Bahaidarah, B. Tanweer, P. Gandhidasan, and S. Rehman, "A combined optical, thermal and electrical performance study of a V-trough PV system-experimental and analytical investigations," *Energies*, vol. 8, no. 4, pp. 2803–2827, 2015, doi: 10.3390/en8042803.

[14]   T. T. Chow, W. He, and J. Ji, "Hybrid photovoltaic-thermosyphon water heating system for residential application," *Sol. Energy*, vol. 80, no. 3, pp. 298–306, 2006, doi: 10.1016/j.solener.2005.02.003.

[15]   A. Shahsavar and M. Ameri, "Experimental investigation and modeling of a direct-coupled PV/T air collector," *Sol. Energy*, vol. 84, no. 11, pp. 1938–1958, 2010, doi: 10.1016/j.solener.2010.07.010.

[16] F. Yazdanifard, E. Ebrahimnia-bajestan, and M. Ameri, "Investigating the performance of a water-based photovoltaic / thermal (PV / T) collector in laminar and turbulent fl ow regime," *Renew. Energy*, vol. 99, pp. 295–306, 2016, doi: 10.1016/j.renene.2016.07.004.

[17] O. Rejeb, H. Dhaou, and A. Jemni, "A numerical investigation of a photovoltaic thermal (PV / T) collector," *Renew. Energy*, vol. 77, pp. 43–50, 2015, doi: 10.1016/j.renene.2014.12.012.

[18] C. Guo, J. Ji, W. Sun, J. Ma, W. He, and Y. Wang, "Numerical simulation and experimental validation of tri-functional photovoltaic / thermal solar collector," *Energy*, pp. 1–11, 2015, doi: 10.1016/j.energy.2015.05.017.

[19] S. Vall and A. Castell, "Radiative cooling as low-grade energy source: A literature review," *Renew. Sustain. Energy Rev.*, vol. 77, no. January, pp. 803–820, 2017, doi: 10.1016/j.rser.2017.04.010.

[20] C. G. Granqvist, A. Hjortsberg, and T. S. Eriksson, "RADIATIVE C O O L I N G TO LOW T E M P E R A T U R E S WITH int," vol. 90, pp. 187–190, 1982.

[21] D. Michell and K. L. Biggs, "Radiation cooling of buildings at night," *Appl. Energy*, vol. 5, no. 4, pp. 263–275, 1979, doi: 10.1016/0306-2619(79)90017-5.

[22] J. Liu, Z. Zhou, J. Zhang, W. Feng, and J. Zuo, "Advances and challenges in commercializing radiative cooling," *Mater. Today Phys.*, vol. 11, p. 100161, 2019, doi: 10.1016/j.mtphys.2019.100161.

[23] M. Zeyghami, D. Y. Goswami, and E. Stefanakos, "A review of clear sky radiative cooling developments and applications in renewable power systems and passive building cooling," *Sol. Energy Mater. Sol. Cells*, vol. 178, no. January, pp. 115–128, 2018, doi: 10.1016/j.solmat.2018.01.015.

[24] X. Lu, P. Xu, H. Wang, T. Yang, and J. Hou, "Cooling potential and applications prospects of passive radiative cooling in buildings : The current state-of-the-art," *Renew. Sustain. Energy Rev.*, vol. 65, no. 4800, pp. 1079–1097, 2016, doi: 10.1016/j.rser.2016.07.058.

[25] Y. Tian, A. Ghanekar, M. Ricci, M. Hyde, O. Gregory, and Y. Zheng, "A review of tunable wavelength selectivity of metamaterials in near-field and far-field radiative thermal transport," *Materials (Basel).*, vol. 11, no. 5, pp. 1–19, 2018, doi: 10.3390/ma11050862.

[26] U. Eicker and A. Dalibard, "Photovoltaic-thermal collectors for night radiative cooling of buildings," *Sol. Energy*, vol. 85, no. 7, pp. 1322–1335, 2011, doi: 10.1016/j.solener.2011.03.015.

[27] M. Hu, G. Pei, Q. Wang, J. Li, Y. Wang, and J. Ji, "Field test and preliminary analysis of a combined diurnal solar heating and nocturnal radiative cooling system," *Appl. Energy*, vol. 179, pp. 899–908, 2016, doi: 10.1016/j.apenergy.2016.07.066.

[28] M. Hu, B. Zhao, X. Ao, Y. Su, Y. Wang, and G. Pei, "Comparative analysis of different surfaces for integrated solar heating and radiative cooling : A numerical study," *Energy*, vol. 155, pp. 360–369, 2018, doi: 10.1016/j.energy.2018.04.152.

[29] M. Hu, B. Zhao, X. Ao, Y. Su, and G. Pei, "Parametric analysis and annual performance evaluation of an air- based integrated solar heating and radiative cooling

collector," vol. 165, 2018.

[30]   S. Vall, A. Castell, and M. Medrano, "Energy Savings Potential of a Novel Radiative Cooling and Solar Thermal Collection Concept in Buildings for Various," pp. 1–10, 2018, doi: 10.1002/ente.201800164.

[31]   S. Vall, K. Johannes, D. David, and A. Castell, "A new flat-plate radiative cooling and solar collector numerical model: Evaluation and metamodeling," *Energy*, vol. 202, 2020, doi: 10.1016/j.energy.2020.117750.

[32]   T. H. Lin, W. C. Hung, and F. S. Sun, "PERFORMANCE EVALUATION OF SOLAR PHOTOVOLTAIC / THERMAL SYSTEMS," vol. 70, no. 5, pp. 443–448, 2001.

[33]   A. Zaite, N. Belouaggadia, C. Abid, B. Hartiti, L. Zahiri, and M. Jammoukh, "Photovoltaic-thermal collectors for night radiative cooling and solar heating: Numerical study," in *Materials Today: Proceedings*, 2019, vol. 30, doi: 10.1016/j.matpr.2020.04.352.

[34]   S. Edition, "Free convection," *Fluid Mech. its Appl.*, vol. 112, pp. 321–338, 2015, doi: 10.1007/978-3-319-15793-1_19.

[35]   T. T. Chow, G. Pei, K. F. Fong, Z. Lin, A. L. S. Chan, and J. Ji, "Energy and exergy analysis of photovoltaic – thermal collector with and without glass cover," *Appl. Energy*, vol. 86, no. 3, pp. 310–316, 2009, doi: 10.1016/j.apenergy.2008.04.016.

[36]   A. M. Saleh, "Modeling of Flat-Plate Solar Collector Operation in Transient States," 2012.

[37]   T. Q. Péan, L. Gennari, B. W. Olesen, and O. B. Kazanci, "Nighttime radiative cooling potential of unglazed and PV / T solar collectors : parametric and experimental analyses," *Proc. 8th Mediterr. Congr. Heating, Vent. Air-conditioning (climamed 2015)*, 2015.

[38]   T. T. Chow, "Performance analysis of photovoltaic-thermal collector by explicit dynamic model," vol. 75, pp. 143–152, 2003, doi: 10.1016/j.solener.2003.07.001.

[39]   G. Heidarinejad, M. Farmahini Farahani, and S. Delfani, "Investigation of a hybrid system of nocturnal radiative cooling and direct evaporative cooling," *Build. Environ.*, vol. 45, no. 6, pp. 1521–1528, 2010, doi: 10.1016/j.buildenv.2010.01.003.

[40]   D. J. and B. W., *Solar engineering of thermal processes*, 3rd editio. New York, 2006.

[41]   E. Ebrahimnia-bajestan, M. Charjouei, and H. Niazmand, "International Journal of Heat and Mass Transfer Experimental and numerical investigation of nanofluids heat transfer characteristics for application in solar heat exchangers," *Int. J. Heat Mass Transf.*, vol. 92, pp. 1041–1052, 2016, doi: 10.1016/j.ijheatmasstransfer.2015.08.107.

[42]   F. P. Incropera and D. P. DeWitt, *Fundamentals of Heat and Mass Transfer*. 1996.

[43]   M. Hu, B. Zhao, X. Ao, Y. Su, and G. Pei, "Numerical study and experimental validation of a combined diurnal solar heating and nocturnal radiative cooling collector," *Appl. Therm. Eng.*, vol. 145, no. January, pp. 1–13, 2018, doi: 10.1016/j.applthermaleng.2018.08.097.

[44]   A. Zaite, N. Belouaggadia, C. Abid, B. Hartiti, and L. Zahiri, "Materials Today : Proceedings Photovoltaic – thermal collectors for night radiative cooling and solar heating : Numerical study," *Mater. Today Proc.*, doi: 10.1016/j.matpr.2020.04.352.

[45] F. Sobhnamayan, F. Sarhaddi, M. A. Alavi, S. Farahat, and J. Yazdanpanahi, "Optimization of a solar photovoltaic thermal (PV / T) water collector based on exergy concept," *Renew. Energy*, vol. 68, pp. 356–365, 2014, doi: 10.1016/j.renene.2014.01.048.

[46] F. Yazdanifard, E. Ebrahimnia-Bajestan, and M. Ameri, "Investigating the performance of a water-based photovoltaic/thermal (PV/T) collector in laminar and turbulent flow regime," *Renew. Energy*, vol. 99, pp. 295–306, 2016, doi: 10.1016/j.renene.2016.07.004.

[47] J. I. Bilbao and A. B. Sproul, "Night Radiative Cooling with Unglazed Pvt-Water Collectors: Experimental Results and Estimation of Cooling Potential," no. December, pp. 1–8, 2017, doi: 10.18086/swc.2015.10.10.